Sustainable Energy, Grids and Networks 38 (2024) 101381

Contents lists available at ScienceDirect

Sustainable Energy, Grids and Networks

journal homepage: www.elsevier.com/locate/segan

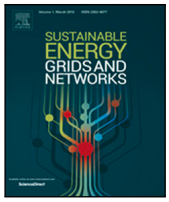

Demand response of an Electric Vehicle charging station using a robust-explicit model predictive control considering uncertainties to minimize carbon intensity

Ana Cabrera-Tobar [a,*], Nicola Blasuttigh [b], Alessandro Massi Pavan [b], Giovanni Spagnuolo [c]

[a] Department of Energy, Politecnico di Milano, 20156 Milan, Italy
[b] Department of Engineering and Architecture, and Center for Energy, Environment and Transport Giacomo Ciamician - University of Trieste, Italy
[c] Department of Information and Electrical Engineering and Applied Mathematics, University of Salerno, Italy

ARTICLE INFO

Keywords:
EV charging stations
Photovoltaic system
Battery energy storage
CO_2 emissions
Two-stage optimization
Robust Optimization
Explicit Model Predictive Control
Real-time operation
Environmental impact
Energy management

ABSTRACT

This paper presents a novel approach to address uncertainties and enable demand response in Electric Vehicle (EV) charging station optimization. A two-stage optimization strategy is proposed, integrating Robust Optimization and explicit Model Predictive Control (eMPC). The first stage involves day-ahead planning using Robust Optimization technique to limit the hourly power consumption of EVs, considering worst-case scenarios caused by uncertainties in EV consumption and CO_2 emissions. The objective is to minimize environmental impact by reducing CO_2 emissions. An Explicit Model Predictive Control strategy is developed in the second stage for real-time operation. The explicit solution, calculated offline, models uncertainties such as the initial state of charge of the battery energy storage, photovoltaic power production, and EV power consumption. During real-time operation, the explicit solution is accessed using measured data from the charging station, refining the schedule derived from the first stage. The proposed solution is implemented and evaluated at an EV charging station in Trieste, Italy. The results demonstrate a significant 69% reduction in CO_2 emissions compared to a deterministic approach while maintaining a real-time computation time of less than 0.1 s.

1. Introduction

1.1. Motivation

To date, there are approximately 1.8 million charging points worldwide. According to [1], the lifecycle emissions of an EV provide a reduction of close to 30% in comparison with a conventional vehicle. In addition, a country with a higher share of renewable energy could help reach a 50% CO_2 emissions reduction during EV usage. Thus, charging stations that are not only fed by the electrical grid but also by renewable energy as photovoltaic (PV) power plants and battery energy storage systems (BESS), could endow a higher reduction of the CO_2 emissions.

Commonly, these charging stations' energy management system (EMS) is focused especially on reducing operational costs, congestion management [2], and energy availability [3]. Still, little attention has been paid to the emissions due to energy use from the grid [4,5]. Due to the random connection of electric vehicles (EVs) to the charging station within electrical systems with variable power generation sources, the environmental benefits of using EVs could be compromised if they are connected during higher energy production from fossil fuels. Thus, limiting the EV's demand regarding emissions, power production from renewable energy, and energy allocation in a BESS [6] is necessary. However, the main challenges for optimal EMS include managing uncertainties such as EV connection/disconnection times and power consumption. Grid-connected charging stations relying on renewable energy face uncertainties related to PV or wind production, state of charge if a BESS is employed, and emissions resulting from grid power consumption.

1.2. Literature survey

Standard optimization techniques commonly used to address uncertainties in EMSs include stochastic, robust, fuzzy, and chance-constrained optimization methods [7–10]. While effective, these techniques can be time-consuming. Therefore, it is preferable to implement them as the initial layer of a multi-stage optimization approach [2,11]. In microgrids, robust optimization emerges as an optimal solution due to its capability to model uncertainties using sets such as polyhedral,

* Corresponding author.
E-mail address: anakarina.cabrera@polimi.it (A. Cabrera-Tobar).

https://doi.org/10.1016/j.segan.2024.101381
Received 31 May 2023; Received in revised form 28 March 2024; Accepted 5 April 2024
Available online 10 April 2024

Nomenclature

η_{bat}	Battery efficiency %
Θ	Space of uncertainties
θ	vector of uncertainties for the second stage of optimization
θ^{ev}	EV's demand uncertainty W
θ^{pv}	PV power production's uncertainty W
θ^{SoC}	SoC's uncertainty %
A, B, C, B_d	coefficient matrices of the state space model
C_{max}	Maximum battery capacity Ws
G, W, E	coefficients of inequalities constraints
i	Time instant for the second stage of optimization
k	Time instant for the first stage of optimization
m	Number of state variables
N	Planning horizon
n	Number of control variables
N_c	Control horizon
P^{bat}	Instantaneous battery power W
P^{bat}_{min}, P^{bat}_{max}	Lower and upper bounds of P_{bat} W
P^{ev}	Instantaneous EV power W
P^{grid}	Instantaneous grid power W
P^{grid}_{min}, P^{grid}_{max}	Lower and upper bounds of P_{grid} W
P^{pv}	Instantaneous PV power W
P_{inv}	Inverter's power W
Q, H, c	Cost function coefficients with the corresponding dimensions
SoC	BESS's state of charge %
SoC^{min}, SoC^{max}	Lower and upper bounds of BESS's SoC %
T_s	Sampling time s
u	Control input variables
w	Vector of Uncertainties for the first stage
w^{eCO_2}	Uncertainty of CO_2 emissions kg/kWh
$w^{eCO_2}_{min}$, $w^{eCO_2}_{max}$	Lower and upper bounds of e^{CO_2} W
w^{ev}	EV power consumption uncertainty W
w^{ev}_{min}, w^{ev}_{max}	Lower and upper bounds of w^{ev} W
x	State space variable

ellipsoids, intervals, etc. Robust Optimization looks for the worst-case scenario by maximizing the uncertainties [12,13]. For instance, the authors in [14] apply Robust Optimization in a microgrid to provide a demand response considering the power generation from renewable energy as uncertainties, which are modeled as cardinal sets. However, online optimization using robust optimization in a real-time charging station can be time-consuming, especially whenever an EV arrives [15].

Therefore, for the second stage optimization, employing a technique that allows for correcting the energy scheduling from the first layer and optimizing in real-time without significant computational overhead is preferable [16]. A promising solution for this purpose is Explicit Model Predictive Control (eMPC) [17]. eMPC enables offline calculation of control laws by defining critical regions, with the limitation of these regions determined by the uncertain parameters' bounds. This technique suits systems like charging stations with few components and uncertain parameters. One of the main advantages of eMPC is its ability to store solutions in a table format that is accessible at any time, making it ideal for real-time operation using less computational time and resources. Despite this advantage, eMPC has received limited attention in the field of EMS [18].

The typical uncertainties considered in the literature are electricity price, power forecast accuracy, and arrival time of the EV. In any of these studies, the environmental aspect is included in the objective function or the uncertain parameters. For instance, the research developed in [10], proposes a chance constraint optimization with a multi-objective approach to reduce the cost and the emissions with a weighting scheme for a microgrid. This study's uncertainties were the PV, wind production, and the load. However, only the effect from natural gas was considered for the emissions, disregarding the electrical grid energy mix. On the other hand, when emissions are considered as part of the objective function for energy scheduling in a microgrid, only a fixed CO_2 emissions coefficient is taken into account, forgetting the variable nature of the current electrical system (e.g. [19,20]).

1.3. Research gap and contributions

In summary, considering uncertainties, the current literature on two-stage optimization for the EMS of a charging station reveals several notable gaps. Firstly, existing studies often lack incorporating a real grid's CO_2 emissions factor as part of the constraints, uncertainties, and objective function. Secondly, there is a noticeable absence of research utilizing robust optimization and explicit model predictive control (eMPC) to provide energy scheduling for limiting energy to electric vehicles (EVs) and reducing purchased power from the grid. Thirdly, various uncertainties such as PV production, grid CO_2 emissions factor, BESS, State of Charge (SoC), and EV consumption for both day-ahead and real-time optimization remain limited. Lastly, there is a deficiency in the availability of easy and practical solutions for real-time operation considering uncertainties. Table 1 compares the present study with similar studies regarding two-stage optimization for the EMS of a charging station, considering uncertainties.

Compared to the existing literature, our study introduces a novel approach to minimize grid electricity purchases and CO_2 emissions in EV charging stations through demand response. While prior research has primarily focused on strategies for optimizing energy management, our methodology integrates both Robust Optimization and eMPC to address uncertainties effectively, enable demand response, and achieve real-time control. The first stage involves day-ahead optimization utilizing adjustable robust optimization to schedule EV charging power and account for uncertainties in EV consumption and variable CO_2 emissions factors. Subsequently, real-time explicit model predictive control (eMPC) is employed to adjust power delivery in response to uncertainties in EV consumption, PV power production, and BESS's SoC. Unlike previous approaches, our framework integrates real-time CO_2 emissions factor and effectively incorporates uncertainties into the optimization process. Thus, the main contributions are as follows:

- Proposal of a two-stage optimization framework using robust optimization and eMPC for real-time control under uncertain conditions.
- Incorporation of uncertainties such as EV consumption, variable CO_2 emissions factors, PV production, and BESS SoC into the energy scheduling process.
- Investigation of computational efficiency and environmental impact reduction through empirical validation at an EV charging station in Trieste, Italy.

The rest of the paper is organized as follows: Section 2 describes the framework of the two-stage optimization. Section 3 explains the robust optimization. Then, the explicit Model Predictive Control is described in Section 4 together with the real-time control. In Section 5, the case studies and the comparison with other methods are described and analyzed. Finally, the conclusions are drawn in Section 6.

Table 1
Summary of the literature review of two-stage optimization for EMS for a microgrid with EVs. (RO: Robust Optimization, SO: Stochastic Optimization, CCO: Chance constraint Optimization, DO: Deterministic Optimization, FO:Fuzzy Optimization, MPC: Model Predictive Control, eMPC: explicit Model Predictive Control).

Reference	Objective function	Optimization techniques	Uncertainty			
			RES power	EV's power	Emissions	BESS' SoC
[14]	Operation cost: operation, maintenance, profit	RO-SO	yes	no	no	no
[10]	Cost and emissions due to natural gas	CCO	yes	yes	no	no
[11]	Operation cost: operation, maintenance, profit	DO-ARO	yes	yes	no	no
[21]	Reduce peak electricity demand	RO-MPC	no	yes	no	no
[22]	Maximize EV's admissions regarding the energy availability	FO-DO	yes	no	no	no
[20]	Minimize operation cost and emissions (fix CO_2 emissions coefficient)	SO-RO	yes	no	no	no
[23]	Maximize profit	SO-RO	yes	no	no	no
[24]	Minimize cost	SO-RO-MPC	yes	yes	no	no
[25]	Operation cost: operation, maintenance, profit	RO-MPC	yes	no	no	no
[26]	Operation cost: operation, maintenance, profit	RO-MILP	yes	no	no	no
[27]	Operation and environmental cost: operation, RES power plants, emissions (fix CO_2 emissions coefficient)	RO-MILP	yes	no	no	no
[28]	Operation cost: operation, maintenance, profit	RO-CCO	yes	yes	no	no
[29]	Operation cost and emissions (fix CO_2 emissions coefficient)	SO-RO	yes	yes	no	yes
This work	Minimize CO_2 emissions	RO-eMPC	yes	yes	yes	yes

2. Two-stage optimization framework

The PV-based charging station considered for the proposed work is shown in Fig. 1. The charging station connects to the grid of the University Campus. The main components are (i) PV modules, (ii) BESS, and (iii) a two-stage inverter. The BESS can be charged using energy from the PV system or, if necessary, from the campus electrical grid. The maximum rated power of the PV/BESS inverter is 3.9 kW. The charging power range of electric vehicles coming to the charging station varies from 3 kW to 22 kW. Because the EVs have different power ranges, the PV/BESS cannot provide all the power the EV needs; thus, the campus grid will supply it. For this reason, as the grid will supply energy to the EV, it is essential to control its consumption depending on the CO_2 emissions generated by the grid energy mix. Thus, smart energy management to reduce its impact is required. The proposed two stage optimization structure for reducing the CO_2 emissions of the charging station is shown in Fig. 2.

For the first stage (day ahead optimization), the inputs are the forecast of the PV power production [30], the CO_2 grid emissions factor (e^{CO_2}) profile, and the BESS's initial state of charge ($SoC_{t=0}$). The technique used for the first stage is Robust Optimization, and it is performed once every 24 h at the beginning of the day. It gives the daily power profile for the grid, the PV panels, and the battery. The output of this stage is the maximum power the charging station can provide to the EV.

In this stage, the main uncertainties are the e^{CO_2} and the EV's charging power (P^{ev}), varying between 0 and 22 kW. The uncertainties are modeled as sets of intervals. For the e^{CO_2}, the set is limited by its minimum and maximum values for the day. Thus, every day these factors will change. Meanwhile, the EV uncertainty set is constructed using its minimum and maximum values. In this stage, PV power production is not considered as an uncertainty due to the accuracy of the forecast.

The e^{CO_2} is calculated for every hour using the forecast of the power generation of the electrical grid in Italy, provided by ENTSO-e service [31]. This factor will determine the emissions caused by the EV's connection to the grid. This factor varies according to the source of the power generation at the electrical grid [32].

Then, the second stage develops any correction to the schedule by considering the maximum values permitted from the day ahead planning. This stage develops the real-time control and also provides an optimal response depending on the future state of charge of the BESS. This control considers the uncertainties as disturbances in real-time. As the optimization for the second stage could be time-consuming, and it is necessary to predict the BESS's SoC for a time horizon, an eMPC.

The following sections explain the problem formulation for each stage and the real-time control.

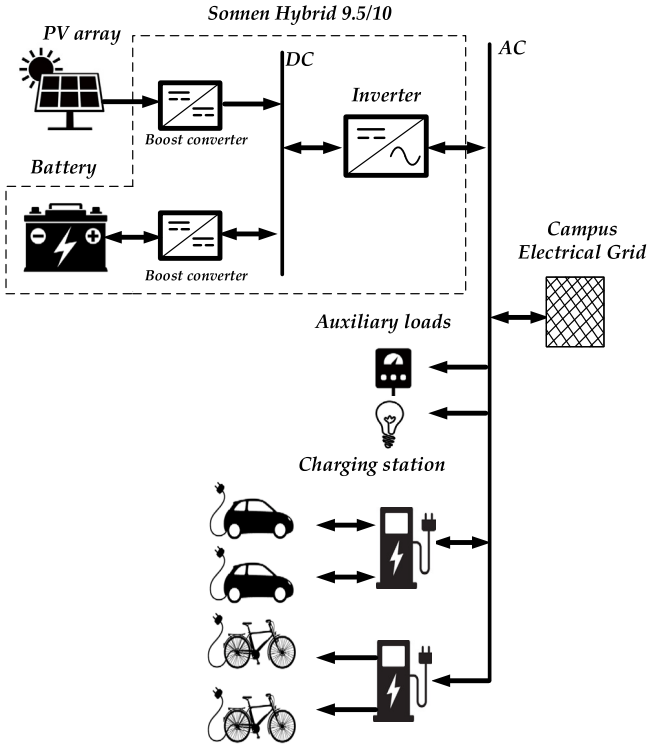

Fig. 1. Schematic of the charging station at the University of Trieste.

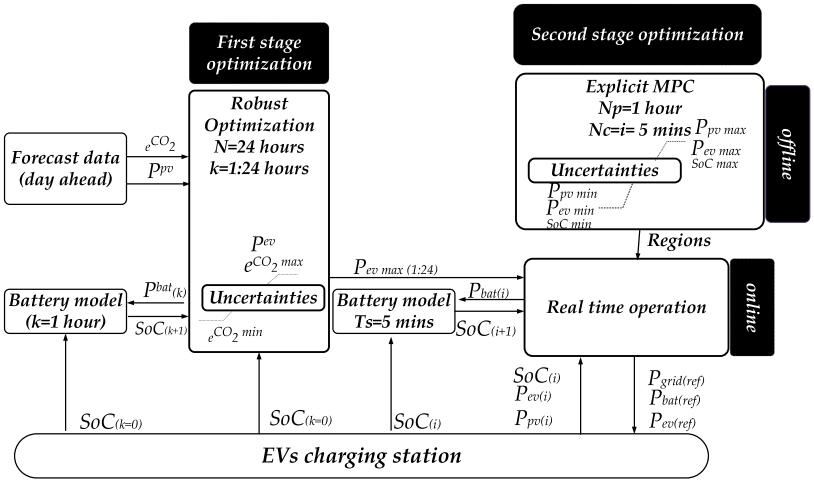

Fig. 2. Proposed EMS considering a two stage optimization.

3. First stage optimization: robust optimization

Robust optimization minimizes an objective function while guaranteeing a set of constraints to be satisfied under the worst-case scenario due to uncertainties. For this purpose, it chooses the best option under a maximization of the uncertainties (min–max objective) [33].

In this section, the problem takes the form of an uncertain discrete linear system:

$$x_{k+1} = Ax_k + Bu_k + B_d w_k, \tag{1}$$

where $x_k \in \mathbb{R}^n$, $u_k \in \mathbb{R}^m$, $w_k \in \mathbb{R}^p$, referring to the state, the control variable and the uncertain disturbances at time step k, respectively. The formulation of the problem is given under a polytopic state and input constraints for a defined planning horizon (N).

$$X = (x_k\ x_{k+1}\ \ldots x_{k+N}),\ \forall W \in \mathbb{W}^N \tag{2}$$

$$U = (u_k\ u_{k+1}\ \ldots u_{k+N-1}),\ \forall W \in \mathbb{W}^N \tag{3}$$

$$W = (w_k\ w_{k+1}\ \ldots w_{k+N}). \tag{4}$$

The function $f(U, W)$ corresponds to the predicted state after k time steps, which varies due to the uncertainties and the control input at each time step. The objective function for a robust optimization takes the form:

$$\min_u \max_w f(U, W) \tag{5}$$

subject to:

$$U \in \mathbb{U}^N,\ \forall W \in \mathbb{W}^N, \tag{6}$$

$$X \in \mathbb{X}^N,\ \forall W \in \mathbb{W}^N, \tag{7}$$

$$W \in \mathbb{W}^N. \tag{8}$$

For the current application, the dynamic of the charging station takes the form presented in Eq. (1), where the state (x_k) represents the BESS's SoC (SoC_k). The control input vector u_k consists of two elements: the battery charging/discharging power (P_k^{bat}) and the power from/to the main grid (P_k^{grid}). The second is a dependent variable of P_k^{bat} and is not directly controllable. The uncertain vector (w_k) contains, as one of its variables, the uncertainty of the EV's power consumption and the time-dependent CO_2 emissions factor $e_k^{CO_2}$. Thus, the vectors appearing in the discrete state space model are:

$$x_k = [SoC_k], \tag{9}$$

$$u_k = \begin{bmatrix} P_k^{bat} & P_k^{grid} \end{bmatrix}, \tag{10}$$

$$w_k = \begin{bmatrix} w_k^{EV} & w_k^{eCO_2} \end{bmatrix}. \tag{11}$$

The dynamic BESS's model calculates the predicted BESS's SoC for the next time step (SoC_{k+1}) with the current measurement of the SoC_k and the ratio between its maximum capacity C_{max} and P_k^{bat} for a determined sampling time (T_s):

$$SoC_{k+1} = SoC_k - \frac{\eta_{bat} T_s}{C_{max}} P_k^{bat}. \tag{12}$$

The dependent control variable (P_k^{grid}) can be determined by the energy balance equation (Eq. (13)). It governs the charging station's operation at each time step (k), ensuring that the sum of the battery power, grid power, and PV power equals the EV power consumption:

$$P_k^{bat} + P_k^{grid} + P_k^{pv} = P_k^{ev}. \tag{13}$$

The objective function looks to minimize the total CO_2 emissions due to the connection of the charging station with the grid when an EV arrives, which depends on the hourly CO_2 emission factor ($e_k^{CO_2}$). The general objective function without uncertainties takes the following form:

$$\min_{p^{grid}} = \sum_{k=0}^{N-1} e_k^{CO_2} \cdot P_k^{grid} \tag{14}$$

s.t

$$SoC^{min} \le SoC_k \le SoC^{max}, \tag{15}$$

$$P_{min}^{grid} \le P_k^{grid} \le P_{max}^{grid}, \tag{16}$$

$$P_{min}^{bat} \le P_k^{bat} \le P_{max}^{bat}. \tag{17}$$

3.1. Uncertainties

The objective function introduced above assumes that $e_k^{CO_2}$ and the EV power consumption is certain. To account for uncertainties, then the objective function has to be minimized under the worst-case scenario due to the uncertainties corresponding to the EV's consumption (w^{ev}) and the CO_2 emissions factor (w^{eCO_2}) respecting the main constraints and the power balance. These uncertainties are modeled as intervals given by $w_k^{ev} \in [P_{min}^{ev}, P_{max}^{ev}]_k$ and $w_k^{eCO_2} \in [e_{min}^{CO_2}, e_{max}^{CO_2}]_k$ that affects the constraints, the state model, the objective function, and the control inputs at every time step ($k = 1, \ldots, N-1$). The intervals are defined by their possible minimum and maximum values. In the case of w^{ev}, the minimum and maximum power values of the EV users for the day are considered. On the other hand, for the w^{eCO_2}, the minimum and maximum values are calculated every day after receiving the grid's power generation forecast from ENTSO-e. With the available data, the e^{CO_2} is calculated for every hour as shown in [32]. Because this is an estimation of the grid's generation, these values cannot be assumed as

certain, and thus, we take only the minimum and the maximum values to set the boundaries of the interval corresponding to w^{eCO_2}.

The problem formulation, including the uncertainties, takes the following form:

$$\min_{p^{grid}} \max_{w_k} = \sum_{k=0}^{N-1} w_k^{eCO_2} \cdot P_k^{grid} \tag{18}$$

s.t

$$P_k^{bat}(w_k) + P^{grid}(w_k)_k + P^{pv}(w_k)_k = P_k^{ev}, \tag{19}$$

$$SoC_{min} \leq SoC_k(w_k) \leq SoC^{max}, \tag{20}$$

$$P_{min}^{grid} \leq P_k^{grid}(w_k) \leq P_{max}^{grid}, \tag{21}$$

$$P_{min}^{bat} \leq P_k^{bat}(w_k) \leq P_{max}^{bat} \tag{22}$$

$$w_{min}^{ev} \leq P_k^{ev} \leq w_{max}^{ev}, \tag{23}$$

$$w_{min}^{eCO_2} \leq e_k^{CO_2} \leq w_{max}^{eCO_2}. \tag{24}$$

The output of the robust optimization corresponds to the optimized values of P_k^{bat} and P_k^{grid} for the worst-case scenario. Then, the maximum value the charging station can provide to the EV is calculated using Eq. (13). Thus, the main output variable from the first stage optimization is the hourly profile of the maximum power to charge the EV ($P_{max_k}^{ev}$), which will be part of the main constraints for the second stage.

4. Second stage optimization: Explicit model predictive control

In the current application, eMPC is used to give the optimal response of the charging station under disturbances. The performance of this eMPC is similar to a conventional MPC, but it adds an extra step because the solution is calculated offline, considering the disturbances as uncertain parameters. The uncertainties are modeled as bounded parameters. The eMPC creates regions of operation that are formed considering the main constraints, the limits of the uncertainties and the value of the objective function. These regions are saved as functions, where the main parameters are uncertainties.

Then, in online mode, at every time step, the control checks the state of the system, SoC, EV, PV and evaluates the regions to get the values for the P^{bat} and the P^{grid}. The formulation of the eMPC is based on the state model of the state of charge of the battery, at every time step (i).

The dynamic discrete model to characterize the operation of the charging station responds to the same equations presented in the previous section (Eqs. (1)–(13)). The state and the control vectors for the discrete model are: $x_i = [SoC_i]$, $u_k = [P_i^{bat}, P_i^{grid}]$. However, for the eMPC formulation, the uncertainties (Θ) considered are the PV power production (θ_i^{pv}), the EV consumption (θ_i^{ev}) and the BESS SoC (θ_i^{SoC}) at every time step i as these parameters influence the eMPC's performance. Thus, the vector state, the control, and the uncertainties vectors are:

$$x_i = [SoC_i], \tag{25}$$

$$u_i = \begin{bmatrix} P_i^{bat} & P_i^{grid} \end{bmatrix}, \tag{26}$$

$$\theta_i = \begin{bmatrix} \theta_i^{pv} & \theta_i^{ev} & \theta_i^{SoC} \end{bmatrix}. \tag{27}$$

The main objective function aims to minimize the use of the grid to provide power to the EV and the BESS when this is discharged, and it is good timing to charge it without causing an increase in emissions. The minimization is calculated for a prediction horizon (N_p). The objective function ($J(i)$) includes the power from the grid, the BESS, and the power from the PV. The EV can charge with a combination of power from these three sources. Furthermore, the grid or the PV modules can also charge the BESS. Thus, the same priority is given to each power source. The objective function is expressed as follows:

$$\min J(i) = \sum_{i=1}^{N_p-1} (P_{grid}^2(i) + (P_{bat}^2(i) + P_{pv}^2(i))). \tag{28}$$

The constraints for the eMPC are the same as the robust optimization detailed in Eq. (14). However, another constraint is added regarding the power limitation provided to the EV, which is limited by the $P_{max_k}^{ev}$ calculated in the first stage ($0 \leq P_i^{ev} \leq P_{max\,k}^{ev}$).

The formulation of the eMPC is based on multiparametric programming (MPP), which solves the problem offline according to the ranges of uncertain parameters [17,34–36]. The objective function, presented in Eq. (28), takes the form of:

$$\begin{aligned} J(\theta) = \min_{u \in \mathbb{R}} \quad & (Qu + H\theta + c)^T u \\ \text{s.t.} \quad & G(\theta)u \leq F + E\theta \\ & \theta \in \Theta \subset \mathbb{R}^q \\ & \theta_l^{min} \leq \theta_l \leq \theta_l^{max}, l = 1, \ldots, q. \end{aligned} \tag{29}$$

On this equation, Θ is the space of the uncertainty parameters, $Q \in \mathbb{R}^{(nxn)}$, $H \in \mathbb{R}^{(nxq)}$, $c \in \mathbb{R}^n$, $G \in \mathbb{R}^{(mxn)}$, $G \in \mathbb{R}^{(mxn)}$, $F \in \mathbb{R}^m$, and $E \in \mathbb{R}^{(mxq)}$. The mathematic transformation is developed using MPT Toolbox from Matlab, and it is explained in [37]. The solution takes the form of:

$$[u(i)] = \alpha \cdot \theta_1(i) + \beta \cdot \theta_2(i) + \gamma \cdot \theta_3(i), \tag{30}$$

where, α, β, and γ are coefficients to determine the control law (CL_i) for a specific value that takes the uncertain parameter in time i.

For the current application, the control law is in function of three uncertainties: (θ_{pv}), (θ_{ev}), (θ_{soc}). The control law takes the following form:

$$[P_i^{bat}\ P_i^{grid}] = \alpha \cdot \theta_i^{pv} + \beta \cdot \theta_i^{ev} + \gamma \cdot \theta_i^{soc}. \tag{31}$$

In MPP formulation, the uncertainties are modeled as intervals. In this case, the uncertainties are limited by their min and maximum value possible: $\theta^{pv} \in [P_{min}^{pv}\ \ P_{max}^{pv}]$, $\theta^{ev} \in [P_{min}^{ev}\ \ P_{max}^{ev}]$ and $\theta^{SoC} \in [SoC_{min}\ SoC_{max}]$.

The output of the second stage is the control variables: P_i^{bat}, P_i^{grid}, and P_i^{ev}. The first two endow the power profile of the charging station, and the last one limits the power to charge the EV.

4.1. Real time control

The control operation of this algorithm happens in various periods of time. The eMPC runs just once in the lifetime of the system and offline. The control laws are saved as a lookup table; the control algorithm can evaluate them anytime. At the beginning of the day (t = 00:00), the state of the charging station is evaluated, which means measuring the BESS's SoC and the EV's power consumption in the case it is connected. Moreover, the daily hourly profiles of the CO_2 emissions and the PV power production are calculated. Then, the robust optimization runs and the maximum EV's, BESS's, and the grid's hourly power profile for the day are calculated and saved. Then, at every time step (i), the values of the uncertain parameters: θ^{pv}, θ^{ev}, θ^{soc} are measured. The first stage of optimization limits the maximum value that can take the uncertainty of θ^{ev}. With the real value, the solution saved by the eMPC is evaluated for the entire N_p, and the corresponding values of P^{bat} and P^{grid} are calculated. The solution sent to the charging station is only for one sampling time. This is repeated every sampling time for all day. The steps for the algorithm are shown in Algorithm 1.

5. Analysis and results

The algorithm developed considering two-stage optimization was evaluated at the charging station in Trieste. The platform is illustrated in Fig. 3, where the Control room communicates with the Transmission System Operator (TSO) by API services, with the different sensors from the PV system using RS485 serial protocol and the EV charging station by the internal University network.

Algorithm 1 Real time control

Run eMPC (one time)
Save Control laws
if $t = 00:00$ **then**
    $CO_2(t = 1:24)$, $P^{pv}(t = 1:24)$
    SoC_{t_0}, $P^{ev}_{t_0}$
    Run Robust optimization
    $u_k \leftarrow P^{grid}_{max\,k}, P^{bat}_{max\,k}$,
    $P^{ev}_{max\,k} \leftarrow P^{grid}_{max\,k} + P^{bat}_{max\,k} + P^{pv}_{k}$,
end if
for i=1:288 **do**
Require: P^{pv}_i, P^{ev}_i, SoC_i
    if $P^{ev}_i \geq P^{ev}_{max\,i}$ **then**
        $P^{ev}_i \leftarrow P^{ev}_{max\,i}$
    else
        $P^{ev}_i \leftarrow P^{ev}_i$
    end if
    Evaluate Control laws
    P^{grid}_i, P^{bat}_i
end for

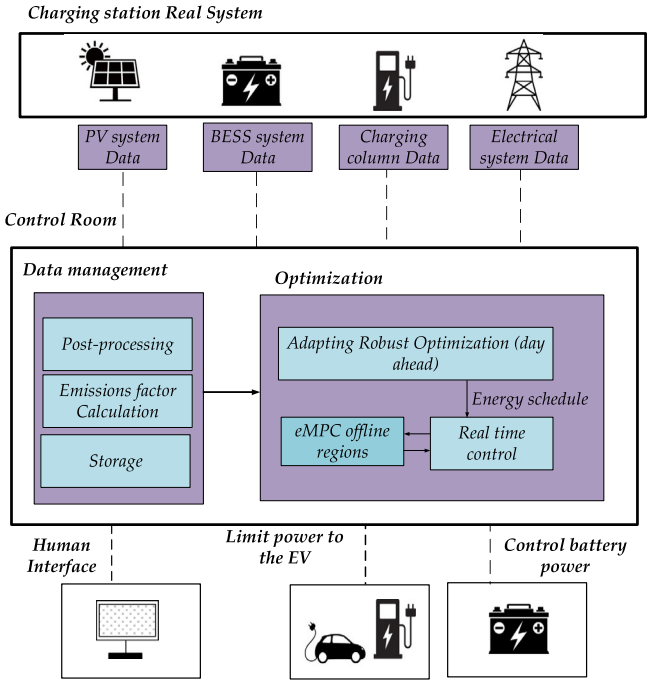

Fig. 3. Control architecture for the proposed EMS.

The robust optimization is calculated daily, which varies depending on the minimum and maximum values of the e^{CO_2} emissions predicted for the day. For this, the Control room communicates with ENTSO-e, which provides the expected power generation for every hour and per type. For the current purpose of this article, the data taken into account will be the Actual Generation per production type, and the country chosen is Italy. The production types stored in this data are biomass, fossil brown coal/lignite, fossil coal-derived gas, fossil gas, hard fossil coal, fossil oil, oil shale, and fossil peat. It also stores data on geothermal, hydro pumped storage, hydro run-of-river, and poundage, hydro water reservoir, marine, nuclear, solar, and wind (onshore and offshore). For the present analysis, oil shale, fossil peat, nuclear, marine, and wind offshore are not considered as these sources have no power for the Italian case. In Italy, fossil brown coal/lignite, fossil coal-derived gas, and hard fossil coal are considered in the same category known as solid [38]. For the case of gas classification, the present study will consider only natural gas.

Table 2
Main parameters of the charging station.

Parameters	Min	Max	Units
P^{grid}	−3.9	22	kW
P^{ev}	0	22	kW
P^{inv}	−4.1	4.1	kW
P^{pv}	0	4.1	kW
P^{bat}	−3.3	3.3	kW
SoC	0	100	%

The monthly variation of the e^{CO_2} is illustrated in Fig. 4, which shows that, for 2019, February was the month with the higher hourly maximum e^{CO_2}, followed by January, October, and November. However, also July shows a maximum e^{CO_2} higher than the other years, close to 0.35 kg/kWh. In 2020, the months with a higher maximum e^{CO_2} were December, February, and March for winter, August for summer, and October for Winter. In 2021, however, the higher maximum e^{CO_2} was from October to December. It can be noticed that during May and June, for the three years, the factor was reduced and reached its minimum (0.1 kg/kWh) in 2019. The factor has been increasing in December, but the average has been reduced in January for these three years. Considering the average values, e^{CO_2} goes from 0.27 to 0.21 from January to May and increases to 0.31 in December for 2021. The same behavior is repeated for the other years, with a negative gradient from January to May and reversing from June to December. Due to this variability, it is important to consider this variation in the EMS for a more environmental decision.

In this article, the analysis of the Robust-eMPC methodology considers the everyday emissions during May 2022 (Fig. 5). As can be seen every day, the emissions factor varies during the day. This can be calculated with the daily ahead power forecast from ENTSO-e. However, this prediction could face some errors due to the variability of electric power demand and generation. Thus, the e^{CO_2} calculated for the current research is an estimation and thus uncertain. Therefore, the Robust optimization optimizes considering the daily estimated e^{CO_2} considering the minimum and maximum value estimated for the day.

Three more case approaches are presented for comparison in the validation of the present algorithm. The case studies are: (i) Normal Operation, (ii) Deterministic Approach, (iii) Robust and Model Predictive Control, and (iv) Robust and Explicit Model Predictive Control (the algorithm proposed in this paper). The description of these approaches is explained in this section. Table 2 presents the corresponding rated power for all the approaches.

For normal operation (NO), the charging station operates with a conventional control that manages the energy from different sources. The control has three orders of priority. The main priority is to charge the EV with the necessary power when it arrives. The power can come from the PV/BESS or the grid. Meanwhile, the second priority is to charge the BESS when PV production is in progress. The PV power is fed into the grid if BESS is fully charged.

For the deterministic approach (DO), the two stages of optimization assume to know the exact time of the EVs connection and the exact e^{CO_2} emissions forecast, together with the PV power production. For the day ahead, linear programming is chosen with the same objective function presented in Eq. (14). For the second stage, a conventional MPC is applied.

For the Robust and conventional MPC (RO-MPC), the first stage of optimization is developed using Robust Optimization (RO) at the beginning of the day. Two main uncertainties are considered: CO_2 emissions and EV power consumption. The connection or disconnection of the EV is unknown. An energy schedule is delivered for the day, focusing on the maximum possible power the charging station can deliver to the EV. The second stage is developed in real-time using a

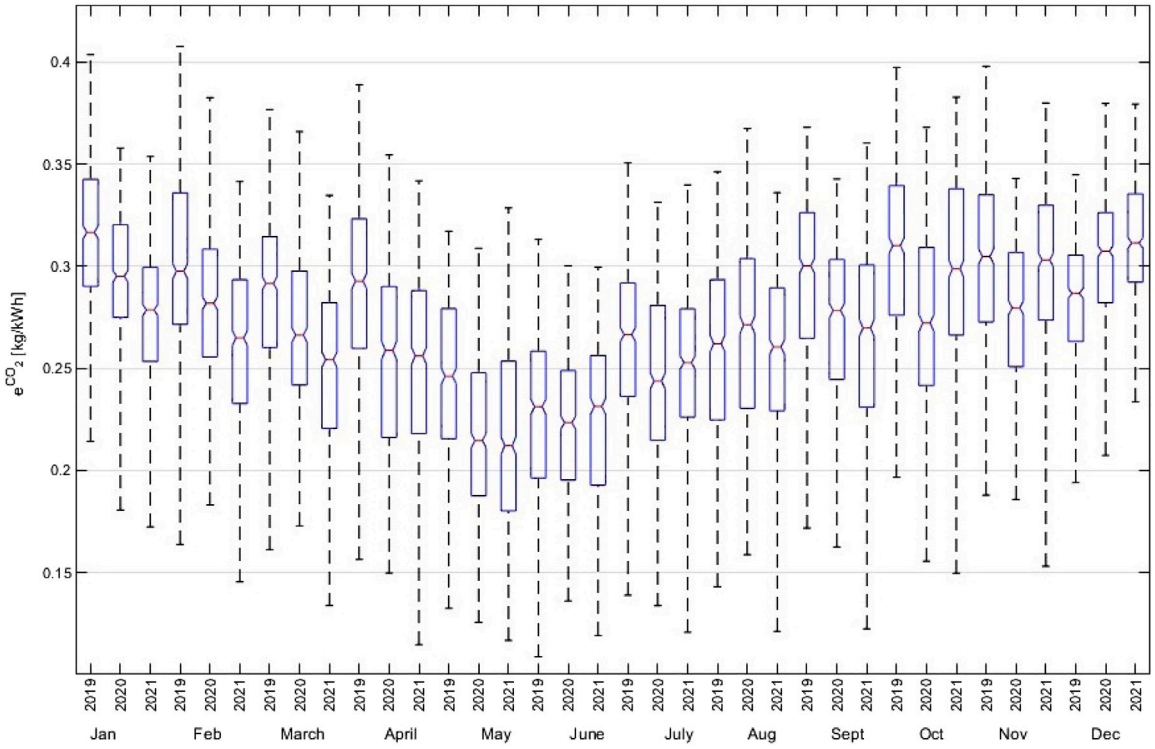

Fig. 4. Box and whiskers plots showing monthly hourly average Emissions factor per month for 2019, 2020, and 2021. In each box, the horizontal line is the median e^{CO_2}, and the box's lower and upper edges are the 25th and 75th percentile, respectively.

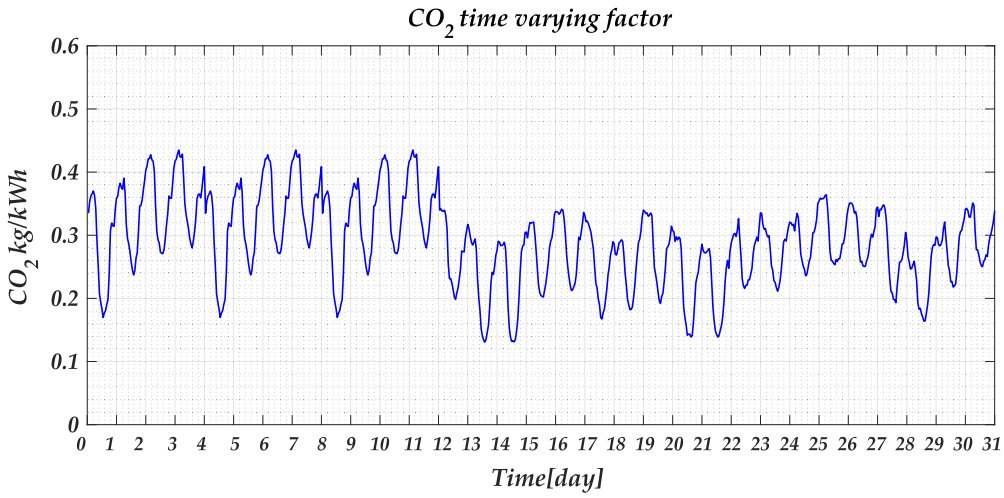

Fig. 5. Variable CO_2 emissions factor due to the electrical grid in Italy (May 2022).

conventional MPC, which uses the problem formulation presented in Eq. (28).

Meanwhile, the last case study considers the current proposed algorithm using Robust Optimization and eMPC (RO-eMPC). Same as in the previous case, the first stage is developed using Robust Optimization to provide the energy schedule of the charging station for the day. In offline mode, the explicit solution of an MPC is calculated for any case scenario. The main uncertainties are PV production, EV consumption, and BESS's SoC. The explicit solution saved offline corresponds to the second stage optimization, which uses the main objective function presented in Eq. (28) but also adding the uncertain parameters (Eq. (27)). The uncertainties for the eMPC are limited by the values presented in Table 3. The explicit solution creates regions as functions of the main uncertainties, as shown in Fig. 6. Then, the decisions are made in real-time, using the actual measurements, searching for the explicit solution of the corresponding region, and then calculating the optimal output.

5.1. Energy analysis

This section presents the energy analysis of the various study cases. We first present the power profile for each of the study cases for one week of May (from the 9th to 13th of May 2022), during which various conditions can be seen: variation of EV arrival time, power consumption, and PV power production. Fig. 7 presents the response for the NO. Table 4 summarizes the total energy delivered to the EV for every studied case.

During normal operation, it can be seen that the EV arrival time is not at night. The University of Trieste set this as mandatory for

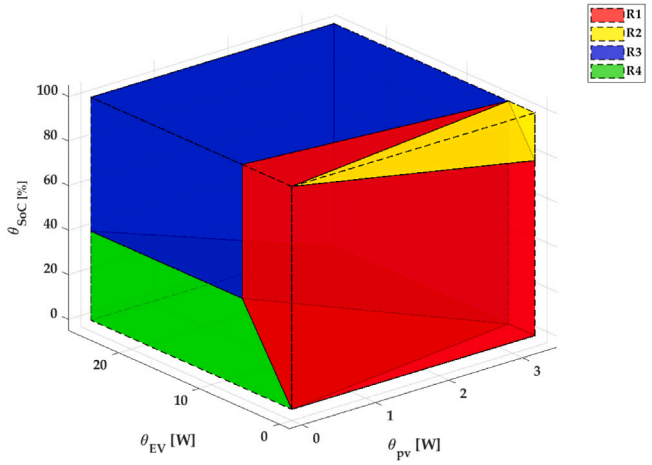

Fig. 6. Regions created using eMPC.

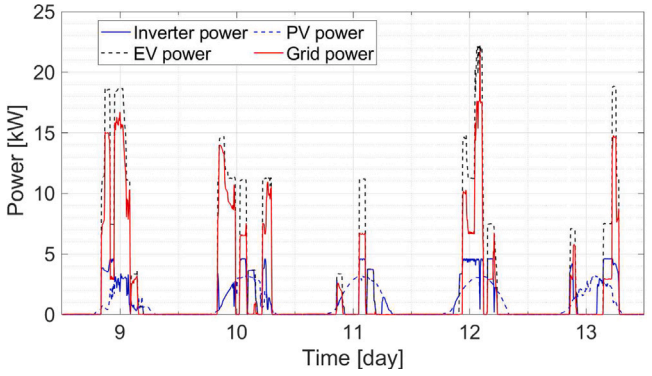

Fig. 7. Power profile of the charging station in normal operation (9th to 13th of May 2022).

the users. As it is a university facility, the EVs do not connect during weekends. During the week analyzed, it can be seen that the EV demand varies randomly from 3 kW to 23 kW. Moreover, four EVs could be connected as maximum at the charging station. The charging station first supplies the power to the EV using the BESS and the PV system. For instance, on the second day (day 10th), there are four different profiles of EV power consumption. The first EV power consumption starts at 8 a.m., consuming power from 14.5 kW, then reduces to 11.26 kW, finishing its charging at 12 p.m. The second EV power consumption starts from 12:30 p.m. to 14:25 p.m. and is 11 kW. Then, a third EV is connected for only two hours in the afternoon from 14:25 p.m. The power required by this EV is 3.6 kW. Finally, the last EV is connected from 17:25 to the end of the day with a power consumption of 11.2 kW.

The maximum power that the inverter provides is 4.1 kW. On the first day, the BESS supplies power to the EV early in the morning. However, as the BESS's SoC is depleted, during the rest of the BESS, the power supplied to the EV uses the power from the PV array and the grid and not from the BESS. Moreover, as the charging station remains busy, the BESS does not charge during the day. Thus, on the second day, the BESS can only provide power after midday as it could charge between 12 and 12:40. The same occurs at the end of the day but could charge completely at any moment. Thus, it gets depleted at the end of the day. Only three EVs were connected to the charging station on the third day. The BESS has time to charge from 10 a.m. to 13:30 p.m.; thus, it can provide energy to the following EVs. As the BESS is completely charged, the surplus of PV production is sent to the grid. The following day, as the BESS is completely charged, the charging station provides a total of 4.1 kW to the EVs, reducing the grid's power consumption. As can be

Table 3
Minimum and maximum values for the main uncertainties considered in the eMPC formulation.

Uncertainties	Min	Max	Units
P^{ev}	0	25	kW
P^{pv}	0	3.9	kW
SoC	0	100	%

Table 4
E^{ev} for every approach (MWh).

Week	NO	DO	RO-MPC	RO-eMPC
2–6 of May	3,44	2,79	1,83	1,83
9–13 of May	4,02	3,38	2,63	2,63
16–20 of May	2,56	2,31	0,82	0,82
23–27 of May	3,03	2,52	1,51	1,51
Total	13,05	11,00	6,79	6,79

seen, when the priority is the load, the BESS is not charged. Because the charging station also depends on the grid, it is necessary that the EV can charge during times with higher renewable energy production in the grid. Thus, leaving it to the BESS to charge with the PV system installed at the university and being used when the grid cannot provide clean energy. Also, it is important to notice that the charging station will consume more power from the grid when the CO_2 emissions intensity factor is higher in the week.

For the DO, the day ahead and the real-time operation are illustrated in Fig. 8a and 8b, respectively. For the day ahead, the power from the grid is limited, considering the exact time the EVs arrive. This power profile is built with the knowledge of the behavior of the EV demand but not the BESS's SoC variation during the day. During the day, the charging station limits the power that it can provide to the EVs. For instance, on the fourth day, the EV power is limited to 11 kW at 12.30 p.m. despite the EVs needing a power of 23 kW. Moreover, the BESS is charged at night, commonly from 2 a.m. until 6 a.m. The PV and the BESS are managed during the real-time operation thanks to the MPC. It can be seen that the BESS supports the delivery of power to the EV and it is charged when the emissions intensity factor is low.

The power profile corresponding to the RO-eMPC is presented in Fig. 9a and Fig. 9b for the day ahead and the real time operation, respectively. The EV's arrival time and power consumption are unknown in this case. The day ahead robust optimization provides a conservative power optimization solution considering the worst-case scenario for EV consumption and CO_2 emissions intensity factor. Compared with DO, this provides the maximum power that can be supplied to the EV every hour and not only at certain times. It is important to notice that during the second week of the test, the EV's power is especially limited during the third day as the e^{CO_2} emissions factor is higher, and the BESS needs to charge for the following days. Then, compared to DO, the power is limited to lower values. Moreover, the day-ahead schedules limited the EV power, depending on the PV power production and the expected variable emissions factor. For instance, on the first day, the charging station can provide power close to 17 kW for various hours during the day in DO. Meanwhile, using RO, the power is limited to less than 10 kW all day, but only at noon; it is permitted to provide a maximum power of 16 kW for a single hour. Then, it reduces to a maximum of 5 kW. However, on Friday 13th, the charging station's maximum power increases per hour, going from 5 kW to 10 kW. This occurs as this day the grid presents a higher emissions factor during the morning, and it reduces at night. During real-time operations using MPC or eMPC, the BESS is used more often than in normal operations or deterministic purposes. It is important to mention that the response of RO-MPC and RO-eMPC are similar; only the computational time varies.

5.2. Environmental impact

The CO_2 emissions factor varies daily, as illustrated in Fig. 5. Thus, the response of the proposed technique in this paper varies depending

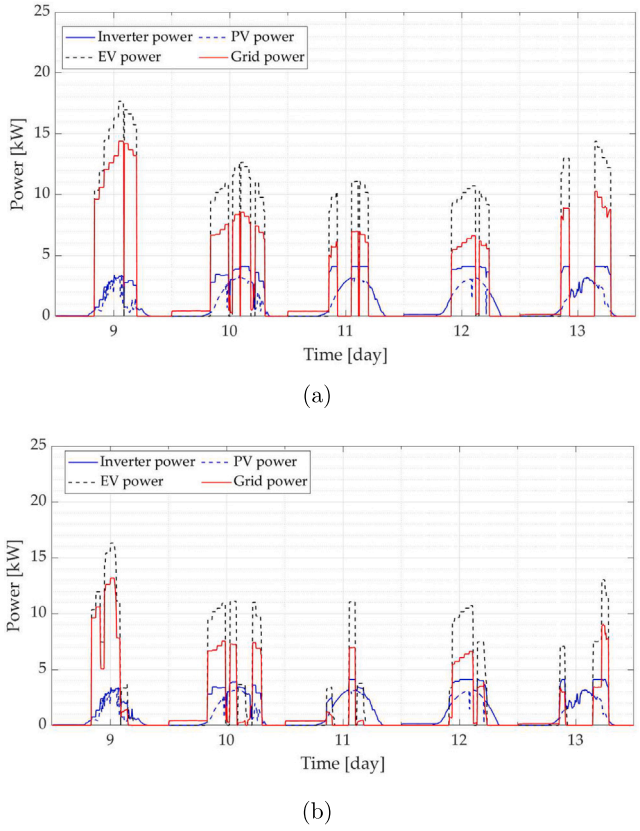

Fig. 8. Power profiles of the charging station for Deterministic Optimization (DO) (9th to 13th of May 2022) (a) Day ahead power profile, (b) real-time optimization using MPC.

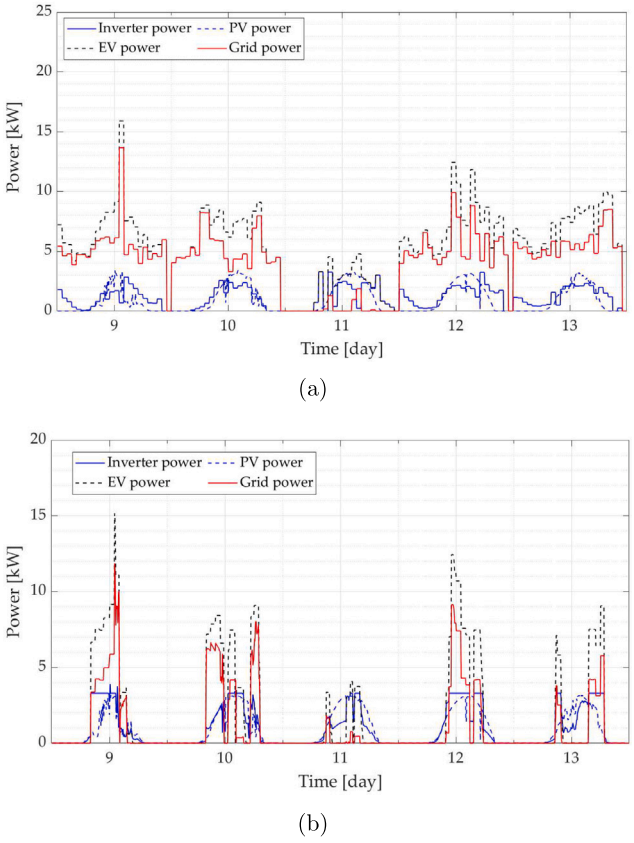

Fig. 9. Power profiles of the charging station for Robust Optimization (RO) (9th to 13th of May 2022) (a) Day ahead power profile, (b) real-time optimization using eMPC.

Table 5
CO_2 emissions generated for every approach ([g]).

Week	NO	DO	RO-MPC	RO-eMPC
2–6 of May	739,96	464,17	110,00	113,00
9–13 of May	735,71	536,88	400,00	402.80
16–20 of May	421,56	297,80	61,50	61,50
23–27 of May	548,47	374,73	179,10	181,20
Total	2445,70	1673,58	750,20	759,00

on the day and the studied case. Table 5 summarizes the emissions for every approach. For instance, during the first week, the CO_2 emissions factor is high, varying from 0.2 to 0.4 kg/kWh. Meanwhile, the variation is from 0.13 to 0.33 kg/kWh during the third week. In normal operation, the microgrid supplies the energy to the EV as required. However, using two-stage optimization, we limit the energy delivered to the EV depending on the variability of the CO_2 emissions factor and the arrival time. Using the proposed algorithm (RO-eMPC), the energy supplied to the EV is reduced by 54% in comparison with normal operation and by about 45%, comparing it with a deterministic approach. In turn, it represents a reduction of 69% in emissions due to the grid's connection. It is important to point out that RO-eMPC approximates the control laws of the RO-MPC, which in response causes a small increase of CO_2 emissions, a maximum of 2% during the first week.

5.3. Computational time

The software used for the simulation is Matlab/Simulink. Meanwhile, the solver for the robust and the eMPC optimization is Yalmip, which also interacts with the MPT 3.0 toolbox [39,40]. Table 6 summarizes the computational time required for each study case. In the first case, the maximum time that the Robust Optimization takes to solve the energy schedule for the day can vary from 13 s to 78 s depending on the available data. However, for the deterministic approach, where all the data are known and assumed as certain, the computational time to calculate the energy schedule for the day can vary between 0.2 s to 4 s. For the second stage optimization, Fig. 10 presents the computational time at every time step MPC or eMPC. The time varies at every time step, depending on the available data. On average, the use of the eMPC represents a reduction of time from 30 to 70% in comparison with a conventional MPC.

Robust Optimization helps generate a possible energy schedule during the day by considering the variable CO_2 emissions factor and the EV's power consumption uncertainty. Although the computation time is higher than a deterministic approach, the main advantage is that it can help reduce the CO_2 emissions due to the grid's connection and provides a realistic energy schedule during the day, considering the possible uncertainties. Moreover, using the eMPC for the second stage optimization helps to have an optimal response when disturbance happens, such as the arrival of the EV, the PV variation, and the BESS's SoC, without affecting the computational time. The eMPC is a good solution for real-time operation, offering to find a solution in less than 0.1 s.

6. Conclusions

This paper presented a demand response of an EV charging station using RO-eMPC considering uncertainties like EV's power consumption and the grid's carbon intensity factor. The solution was implemented in a real charging station located at the University of Trieste in Italy. The conclusions can be drawn as follows.

Table 6
Computational time for the first stage optimization [s].

Week	Day 1		Day 2		Day 3		Day 4		Day 5	
	RO	DO	RO	DO	RO	DO	RO	DO	RO	DO
2–6 of May	34.5	4	33	0.6	29	0.5	26	0.4	19	0.6
9–13 of May	38.9	0.6	78	0.5	51	0.4	55	0.4	38	0.6
16–20 of May	17.1	0.3	22	0.4	15	0.3	12	0.3	17	0.2
23–27 of May	13.3	0.2	18	0.4	15	0.3	13	0.3	17	0.2

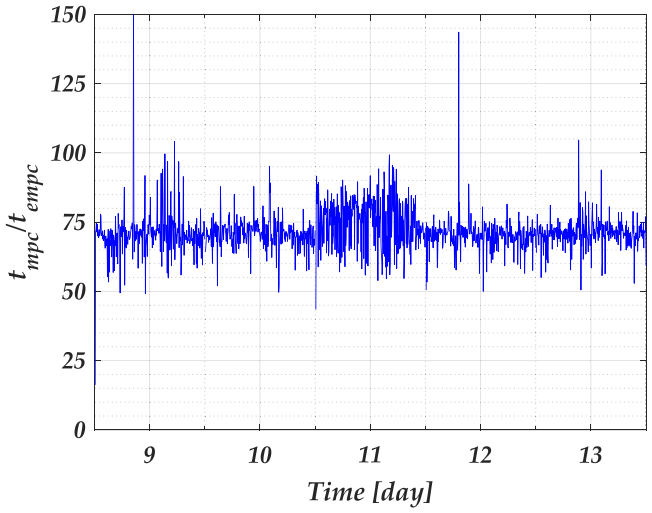

Fig. 10. Ratio of the computational time for every time step to run MPC and eMPC (9th to 13th of May 2022). The time MPC takes to solve the online optimization varies from 50 to 150 times more than with eMPC.

To manage uncertainties, we proposed a two-stage optimization that is easy to implement in a real charging station. The first stage was a robust optimization that runs every day, using information from the utility service concerning the forecasted power generation from the grid. Then, the expected carbon intensity factor from the grid is calculated. Then, the robust optimization adapts the bounds of the uncertainty regarding the carbon intensity factor and searches for the optimal energy schedule for the charging station, focused especially on the total power that can be provided to the EVs to have less carbon emission footprint for the day.

The second stage was developed to run in online mode but reducing the computational time. Thus, eMPC was used for this stage because its operation is similar to a conventional MPC, but its solution was calculated offline, considering uncertainties such as PV production, EV power consumption, and the BESS's SoC.

The solution proposed in this article has been easy to implement and adapt to the real charging station located at the University of Trieste. The control algorithm could run in real time taking into account the energy schedule and the optimal energy management. As the eMPC only needs to enter the critical regions, no special computational platform is needed to run it, and it only needs 0.1 s to provide an optimal response. Moreover, the robust optimization was also easy to implement and only took 13 s to 78 s to provide an energy schedule for the day. The results showed that with this approach, the CO_2 emissions were reduced by about 69% as the energy delivered to the EV was limited by the energy schedule optimal calculated by the Robust Optimization. Compared with other studies in the area, this study was the first to consider a variable carbon intensity factor considering the grid power generation variability.

Funding

This work was supported by "MUSE—Cross-border collaboration for a sustainable and energetically efficient university mobility", co-financed by the ERDF via the cross-border cooperation program Interreg Italy-Slovenia, and by "DEEP-SEA - Development of energy efficiency planning and services for the mobility of Adriatic Marinas". This research was also funded by the "Ministero dell'Università e Ricerca" in the frame of PRIN 2017 project: HEROGRIDS (#2017WA5ZT3_003), and by FARB funds of the University of Salerno.

CRediT authorship contribution statement

Ana Cabrera-Tobar: Conceptualization, Formal analysis, Investigation, Methodology, Software, Validation, Writing – original draft, Writing – review & editing. **Nicola Blasuttigh:** Software, Validation, Writing – review & editing. **Alessandro Massi Pavan:** Conceptualization, Funding acquisition, Project administration, Supervision, Writing – review & editing. **Giovanni Spagnuolo:** Conceptualization, Formal analysis, Funding acquisition, Methodology, Project administration, Supervision, Writing – review & editing.

Declaration of competing interest

The authors declare that they have no known competing financial interests or personal relationships that could have appeared to influence the work reported in this paper.

Data availability

Data will be made available on request.

References

[1] Global EV Outlook 2020, Tech. Rep., IEA, Paris, 2020, URL https://www.iea.org/reports/.
[2] Q. Yan, B. Zhang, M. Kezunovic, Optimized operational cost reduction for an EV charging station integrated with battery energy storage and PV generation, IEEE Trans. Smart Grid 10 (2) (2019) 2096–2106, http://dx.doi.org/10.1109/TSG.2017.2788440.
[3] Y. Wang, J.S. Thompson, Two-stage admission and scheduling mechanism for electric vehicle charging, IEEE Trans. Smart Grid 10 (3) (2019) 2650–2660, http://dx.doi.org/10.1109/TSG.2018.2807158.
[4] N. Blasuttigh, S. Pastore, M. Scorrano, R. Danielis, A. Massi Pavan, Vehicle-to-ski: A V2G optimization-based cost and environmental analysis for a ski resort, Sustain. Energy Technol. Assess. (2022).
[5] D. Mazzeo, Nocturnal electric vehicle charging interacting with a residential photovoltaic-battery system: a 3E (energy, economic and environmental) analysis, Energy 168 (2019) 310–331, http://dx.doi.org/10.1016/j.energy.2018.11.057.
[6] M.A. Beyazıt, A. Taşcıkaraoğlu, J.P. Catalão, Cost optimization of a microgrid considering vehicle-to-grid technology and demand response, Sustain. Energy Grids Netw. 32 (2022) 100924, http://dx.doi.org/10.1016/J.SEGAN.2022.100924.
[7] J. Guo, Y. Lv, H. Zhang, S. Nojavan, K. Jermsittiparsert, Robust optimization strategy for intelligent parking lot of electric vehicles, Energy 200 (2020) 117555, http://dx.doi.org/10.1016/j.energy.2020.117555.
[8] X. Wu, X. Hu, X. Yin, S.J. Moura, Stochastic optimal energy management of smart home with PEV energy storage, IEEE Trans. Smart Grid 9 (3) (2018) 2065–2075, http://dx.doi.org/10.1109/TSG.2016.2606442.
[9] S. Faddel, A.T. Al-Awami, M.A. Abido, Fuzzy optimization for the operation of electric vehicle parking lots, Electr. Power Syst. Res. 145 (2017) 166–174, http://dx.doi.org/10.1016/j.epsr.2017.01.008.

[10] G. Zhu, Y. Gao, H. Sun, Optimization scheduling of a wind–photovoltaic–gas–electric vehicles community-integrated energy system considering uncertainty and carbon emissions reduction, Sustain. Energy Grids Netw. 33 (2023) 100973, http://dx.doi.org/10.1016/J.SEGAN.2022.100973.

[11] J. Wu, Y. Liu, X. Chen, C. Wang, W. Li, Data-driven adjustable robust day-ahead economic dispatch strategy considering uncertainties of wind power generation and electric vehicles, Int. J. Electr. Power Energy Syst. 138 (2022) 107898, http://dx.doi.org/10.1016/J.IJEPES.2021.107898.

[12] A. Vaccaro, M. Petrelli, A. Berizzi, Robust optimization and affine arithmetic for microgrid scheduling under uncertainty, in: Proceedings - 2019 IEEE International Conference on Environment and Electrical Engineering and 2019 IEEE Industrial and Commercial Power Systems Europe, EEEIC/I and CPS Europe 2019, Institute of Electrical and Electronics Engineers Inc., 2019, http://dx.doi.org/10.1109/EEEIC.2019.8783572.

[13] B. Zhang, Q. Li, L. Wang, W. Feng, Robust optimization for energy transactions in multi-microgrids under uncertainty, Appl. Energy 217 (2018) 346–360, http://dx.doi.org/10.1016/J.APENERGY.2018.02.121.

[14] H. Xiao, F. Long, L. Zeng, W. Zhao, J. Wang, Y. Li, Optimal scheduling of regional integrated energy system considering multiple uncertainties and integrated demand response, Electr. Power Syst. Res. 217 (2023) 109169, http://dx.doi.org/10.1016/J.EPSR.2023.109169, URL https://linkinghub.elsevier.com/retrieve/pii/S0378779623000585.

[15] X. Yue, S. Pye, J. DeCarolis, F.G. Li, F. Rogan, B. Gallachóir, A review of approaches to uncertainty assessment in energy system optimization models, Energy Strategy Rev. 21 (2018) 204–217, http://dx.doi.org/10.1016/j.esr.2018.06.003.

[16] M. Elkazaz, M. Sumner, D. Thomas, Energy management system for hybrid PV-wind-battery microgrid using convex programming, model predictive and rolling horizon predictive control with experimental validation, Int. J. Electr. Power Energy Syst. 115 (2020) 105483, http://dx.doi.org/10.1016/j.ijepes.2019.105483.

[17] A. Cabrera-Tobar, A. Massi Pavan, N. Blasuttigh, G. Petrone, G. Spagnuolo, Real time energy management system of a photovoltaic based e-vehicle charging station using explicit model predictive control accounting for uncertainties, Sustain. Energy Grids Netw. 31 (2022) 100769, http://dx.doi.org/10.1016/J.SEGAN.2022.100769.

[18] I. Pappas, D. Kenefake, B. Burnak, S. Avraamidou, H.S. Ganesh, J. Katz, N.A. Diangelakis, E.N. Pistikopoulos, Multiparametric programming in process systems engineering: Recent developments and path forward, Front. Chem. Eng. (2021) 32, http://dx.doi.org/10.3389/FCENG.2020.620168.

[19] B. Dey, S. Misra, F.P. Garcia Marquez, Microgrid system energy management with demand response program for clean and economical operation, Appl. Energy 334 (2023) 120717, http://dx.doi.org/10.1016/J.APENERGY.2023.120717.

[20] Y.P. Xu, R.H. Liu, L.Y. Tang, H. Wu, C. She, Risk-averse multi-objective optimization of multi-energy microgrids integrated with power-to-hydrogen technology, electric vehicles and data center under a hybrid robust-stochastic technique, Sustainable Cities Soc. 79 (2022) 103699, http://dx.doi.org/10.1016/J.SCS.2022.103699.

[21] R. Ghotge, Y. Snow, S. Farahani, Z. Lukszo, A. van Wijk, Optimized scheduling of EV charging in solar parking lots for local peak reduction under EV demand uncertainty, Energies 13 (5) (2020) http://dx.doi.org/10.3390/en13051275.

[22] Y. Wang, J.S. Thompson, Two-stage admission and scheduling mechanism for electric vehicle charging, IEEE Trans. Smart Grid 10 (3) (2019) 2650–2660, http://dx.doi.org/10.1109/TSG.2018.2807158.

[23] A. Baringo, L. Baringo, A stochastic adaptive robust optimization approach for the offering strategy of a virtual power plant, IEEE Trans. Power Syst. 32 (5) (2017) 3492–3504, http://dx.doi.org/10.1109/TPWRS.2016.2633546.

[24] Z. Ji, X. Huang, C. Xu, H. Sun, Accelerated model predictive control for electric vehicle integrated microgrid energy management: A hybrid robust and stochastic approach, Energies 9 (11) (2016) 973, http://dx.doi.org/10.3390/en9110973, URL http://www.mdpi.com/1996-1073/9/11/973.

[25] H. Qiu, W. Gu, Y. Xu, B. Zhao, Multi-time-scale rolling optimal dispatch for AC/DC hybrid microgrids with day-ahead distributionally robust scheduling, IEEE Trans. Sustain. Energy 10 (4) (2019) 1653–1663, http://dx.doi.org/10.1109/TSTE.2018.2868548.

[26] J. Yang, C. Su, Robust optimization of microgrid based on renewable distributed power generation and load demand uncertainty, Energy 223 (2021) 120043, http://dx.doi.org/10.1016/J.ENERGY.2021.120043.

[27] Z. Siqin, D.X. Niu, X. Wang, H. Zhen, M.Y. Li, J. Wang, A two-stage distributionally robust optimization model for P2G-CCHP microgrid considering uncertainty and carbon emission, Energy 260 (2022) 124796, http://dx.doi.org/10.1016/J.ENERGY.2022.124796.

[28] H. Xie, S. Gao, J. Zheng, X. Huang, A three-stage robust dispatch model considering the multi-uncertainties of electric vehicles and a multi-energy microgrid, Int. J. Electr. Power Energy Syst. 157 (2024) 109778, http://dx.doi.org/10.1016/J.IJEPES.2023.109778.

[29] Q. Guo, X. Liang, D. Xie, K. Jermsittiparsert, Efficient integration of demand response and plug-in electrical vehicle in microgrid: Environmental and economic assessment, J. Clean. Prod. 291 (2021) 125581, http://dx.doi.org/10.1016/J.JCLEPRO.2020.125581.

[30] S. Negri, F. Giani, A. Massi Pavan, A. Mellit, E. Tironi, MPC-based control for a stand-alone LVDC microgrid for rural electrification, Sustain. Energy Grids Netw. 32 (2022) 100777, http://dx.doi.org/10.1016/J.SEGAN.2022.100777.

[31] ENTSO-E, URL https://www.entsoe.eu/.

[32] A. Cabrera-Tobar, N. Blasuttigh, A. Massi Pavan, V. Lughi, G. Petrone, G. Spagnuolo, Energy scheduling and performance evaluation of an e-vehicle charging station, Electronics 2022, Vol. 11, Page 3948 11 (23) (2022) 3948, http://dx.doi.org/10.3390/ELECTRONICS11233948.

[33] J. Löfberg, Minimax Approaches to Robust Model Predictive Control, (no. 812) 2003, URL http://www.control.isy.liu.se.

[34] S. Gerkšič, Improving reliability of partition computation in explicit MPC with MPT toolbox, IFAC Proc. Vol. 44 (1) (2011) 9260–9265, http://dx.doi.org/10.3182/20110828-6-IT-1002.02454.

[35] A. Alessio, A. Bemporad, A survey on explicit model predictive control, in: Lecture Notes in Control and Information Sciences, Springer, Heidelberg, http://dx.doi.org/10.1007/978-3-642-01094-1_29.

[36] R. Oberdieck, N.A. Diangelakis, I. Nascu, M.M. Papathanasiou, M. Sun, S. Avraamidou, E.N. Pistikopoulos, On multi-parametric programming and its applications in process systems engineering, Chem. Eng. Res. Des. 116 (2016) 61–82, http://dx.doi.org/10.1016/j.cherd.2016.09.034.

[37] A. Bemporad, M. Morari, V. Dua, E.N. Pistikopoulos, Explicit solution of model predictive control via multiparametric quadratic programming, in: Proceedings of the American Control Conference, vol. 2, IEEE, 2000, pp. 872–876, http://dx.doi.org/10.1109/acc.2000.876624.

[38] A.A.B. Ruíz, Fattori di emissione atmosferica di gas a effetto serra e altri gas nel settore elettrico, vol. 3, (no. 2) 2015, pp. 54–67, URL http://repositorio.unan.edu.ni/2986/1/5624.pdf.

[39] J. Löfberg, Automatic robust convex programming, 27 (1), (ISSN: 10556788) 2010, pp. 115–129, http://dx.doi.org/10.1080/10556788.2010.517532.

[40] M. Herceg, M. Kvasnica, C.N. Jones, M. Morari, Multi-parametric toolbox 3.0, in: 2013 European Control Conference, ECC 2013, 2013, pp. 502–510, http://dx.doi.org/10.23919/ecc.2013.6669862.